Pergamon

0043-1354(95)00110-7

Wat. Res. Vol. 30, No. 1, pp. 29–36, 1996

0043-1354/96 $9.50 + 0.00

EFFECTS OF SHEAR STRESS AND SUBSTRATE LOADING RATE ON *PSEUDOMONAS AERUGINOSA* BIOFILM THICKNESS AND DENSITY

BRENT M. PEYTON

Pacific Northwest Laboratory*, P.O. Box 999, Richland, WA 99352, U.S.A.

(First received November 1994; accepted in revised form April 1995)

Abstract—Thickness, roughness, and density data were obtained from monopopulation *Pseudomonas aeruginosa* biofilms grown in an annular reactor under different substrate loading rates and shear stresses. Biofilm thickness showed significant increases, up to approx. 30 μm, with increasing substrate loading rate. Shear stress had no significant effect on thickness. Biofilm roughness, as measured by the standard deviation of the thickness, increased with increasing thickness. Areal mass density significantly increased with substrate loading rate and was not significantly affected by shear stress. Substrate loading and shear stress did not significantly affect volumetric mass density. A numerical expression that describes changes volumetric density as a function of biofilm depth is presented.

Key words—Biofilm, *Pseudomonas aeruginosa*, accumulation, measurement, thickness, density, shear stress, substrate loading

NOMENCLATURE

$k_{\rho 1}$ = first order density coefficient in equation (1) (M L^{-3})
$k_{\rho 1/2}$ = one-half order density coefficient in equation (2) (M L$^{-5/2}$)
L_f = biofilm thickness (L)
L_{fm} = monolayer biofilm thickness (L)
X_f = areal biofilm density (M L^{-2})
z = location in biofilm perpendicular to the substratum (L)
ρ_f = average volumetric biofilm density (M L^{-3})
ρ_{fm} = volumetric biofilm density of a monolayer (M L^{-3})
ρ_z = local volumetric biofilm density (M L^{-3})

INTRODUCTION

A biofilm is a matrix of cells and cellular products attached to a solid surface or substratum. Biofilms grow, reproduce, and produce extracellular polymers and other byproducts. They are found in most natural and industrial aquatic systems and account for much of the overall microbial activity in these systems. Wuhrmann (1971) estimated that 90–99.99% of the bacterial activity in shallow streams is associated with biofilms. In addition, biofilms have a significant influence in public health with regard to contamination of drinking water (LeChevallier *et al.*, 1987, 1991; van der Wende *et al.*, 1989) and bacterial infections of living tissue, teeth, prosthetic devices, and contact lenses (Richards and Gagnon 1993, Gagnon and Richards 1993, Olsson *et al.*, 1992; Duguid *et al.*, 1992; Wilson *et al.*, 1990).

Many deleterious effects of biofilm formation have been reported in industrial systems, consequently, biofilm research is usually aimed at reducing fouling from unwanted biofilms. Biofilm accumulation reduces heat transfer efficiency in heat exchangers and condensers (Characklis *et al.*, 1980). Geesey and colleagues (1987) examined the biological plugging of oil sand reservoirs to determine whether a water source would induce biofilm accumulation and consequent plugging of the formation. In oilfields, biofilm accumulation and plugging around injection wells results in decreased injection rate or higher injection pressure. Biofilm plugging has also been implicated in the closure of nutrient injection wells for *in situ* bioremediation (Semprini *et al.*, 1991; Shouche *et al.*, 1993). The use of biofilm reactors had led to the rapidly increasing application of *ex situ* bioremediation such as vapor phase bioreactors (Shields *et al.*, 1994; Saberiyan *et al.*, 1994) and packed and fluidized beds (Mulcahy *et al.*, 1987; Chang *et al.*, 1991; Voice *et al.*, 1992).

Better characterization of biofilm properties can enhance understanding of the process and accurate quantitative description of the system. However, only limited parameters are currently available for a quantitative description of biofilm accumulation. Two variables that are commonly used to help characterize the accumulation of a biofilm are its thickness and areal density. A third variable, roughness, describes the standard deviation of the thickness and helps to characterize the spatial heterogeneity within a

*Pacific Northwest Laboratory is operated for the U.S. Department of Energy by Battelle Memorial Institute under contract DE-AC06-76RLO 1830.

biofilm. To better define the effects of environmental influences on thickness, roughness, and density, this paper presents data obtained from a monopopulation *Pseudomonas aeruginosa* biofilm grown in an annular reactor under different substrate loading rates and shear stresses, and presents a numerical expression that describes volumetric density as a function of biofilm depth.

Biofilm thickness, the perpendicular distance from the substratum to the biofilm-bulk liquid interface, has been historically used to determine the distance through which substrates and nutrients must diffuse to fully penetrate a biofilm. This one-dimensional view of a biofilm is being expanded with new data (Bryers and Drummond, 1995) which suggest that convection may be a significant mechanism for nutrient mass transport in heterogenous biofilms. In addition, diffusion into biofilm colonies may be slower than previously reported. These micro-scale observations enhance our understanding of the complexities of biofilm processes; however, until numerical simulations can incorporate this increased complexity, average values of biofilm thickness and diffusivity must still be used for macro-scale modelling and design purposes. Whether a biofilm is dominated by either diffusion or convection, the thickness is still an important characteristic for both fundamental and applied biofilm research.

Biofilm thickness negatively influences fluid frictional losses and heat transfer resistances in industrial process equipment and is the primary variable that determines the plugging of porous media for *in situ* bioremediation (Jennings *et al.*, 1994). Thickness has been measured primarily by three methods: optical, volumetric displacement, and electrical conductance. The optical method, which requires a transparent substratum and a light microscope with a micrometer focus, was developed by Sanders (1964) and refined by Bakke and Olsson (1986). The volumetric displacement method, first reported by Picologlou *et al.* (1980) and was used by Turakhia and Characklis (1983), entails measuring the volumetric displacement of a biofilm covered substratum, scraping the biofilm from the substratum, and determining the volume of the clean substratum. Measurement of biofilm thickness by electrical conductance, reported by Norrman *et al.* (1977) for use in metal pipes or on metal biofilm coupons, uses a micrometer and steel needle electrode to determine when an electrical circuit is completed. The pipe or coupon is drained of water and connected to the electrical circuit. As the needle is lowered onto the biofilm, a small current begins to flow through the circuit. When the needle touches the metal substratum, the current becomes significantly larger. The difference in the micrometer readings is the biofilm thickness.

Volumetric displacement provides the average thickness over the measured area; whereas the optical and electrical methods give point measurements at specific locations. Many optical or electrical measurements are required to defined the average biofilm thickness in a statistically accurate manner. However, data obtained from different locations provide information on the "roughness" that cannot be measured by volumetric displacement. Roughness is defined here as the standard deviation of eight optical-thickness measurements, but has been defined elsewhere as the average height of surface projections relative to some datum (Cunningham, 1989). Roughness is particularly high in undefined populations, where biofilm thicknesses are large and can exhibit spatially significant variation even under conditions of constant substrate loading and shear stress (Peyton, 1992). In monopopulation biofilms, both the thickness and the variation of the thickness is usually less than in mixed populations (Christensen and Characklis, 1990).

Areal density is the amount of dry biomass which is attached to a unit area of substratum. Areal density depends on environmental conditions and is, in general, reported less often than volumetric density. Volumetric density is the amount of biomass in a given volume of biolfilm and is reported as dry biomass per unit wet volume (Table 1). Volumetric density is important in the mathematical modeling of biofilm processes, since biomass concentration is often related to the activity of a biofilm. The only data available on the variation of biofilm density with biofilm depth is by Masuda *et al.* (1991), given in Table 2, who used a "microslicer" to section the biofilm and measure the density for each section. Volumetric density has been correlated with shear stress. Characklis *et al.* (1980) reported increasing biofilm density with increasing shear stress at low

Table 1. Previously reported values of biofilm volumetric mass density (ρ_f) and thickness (L_f)

Type[a]	Volumetric biofilm density ($kg\,m^{-3}$)	Thickness (10^{-6} m)	Reference
A	66–130	160–210	(Kornegay and Andrews, 1967)
A	50[n]	100	(Rittmann and McCarty, 1978)
A	12–78[b]	7–32	(Chang *et al.*, 1991)
B	20–105	30–1300	(Hoehn and Ray, 1973)
B	5[c]	119–126	(Herbert, 1976)
B	5[c]	0–125	(Rittmann and McCarty, 1980)
B	10–65	10–124	(Trulear and Characklis, 1982)
C	42–109	150–580	(Williamson and McCarty, 1976)
D	27	0–60	(Bakke, 1983)

[a]A: steady state, heterotrophic mixed population; B: heterotrophic mixed population; C: steady state, nitrifying mixed population; D: steady state, *Pseudomonas aeruginosa*.
[b]Calculated assuming biofilm is 80% volatile solids.
[c]Calculated assuming biofilm is 50% carbon.

Table 2. Volumetric mass density (ρ_f) with biofilm depth (Masuda *et al.*, 1991)

Film morphology	Volumetric density (10^3 dry $g\,m^{-3}$)	Depth from bulk liquid–biofilm interface (10^{-6} m)	Thickness of biofilm section (10^{-6} m)
Surface film	37	0–400	400
Intermediate	98	400–600	200
Base film	102	600–730	130

substrate-loading rates. On the other hand, Kornegay and Andrews (1967) showed that biofilm density did not change with changes in shear stress at high substrate loading rates. Determining the relationship of substrate loading rate and shear stress on volumetric density is required for more accurate computer simulation of biofilm–system behavior.

Biofilms are reported to have two compartments, surface film and base film, and may consist entirely of one compartment or a combination of both (Wilderer and Characklis, 1989). Suschka (1987) postulated the existence of a surface film with a different porosity than that of the base film. A three-fold difference in experimentally measured and theoretically calculated residence times in trickling filters led to the conclusion that there must be two liquid film layers: "free" liquid flowing over the top of the biofilm and a "captured" layer flowing within the biofilm. The surface film is the heterogeneous region near the biofilm/bulk-liquid interface and is characterized by a rough, visco-elastic surface. In turbulent flow, surface morphology may contribute significantly to fluid friction (Picologlou *et al.*, 1980) and advective transport may dominate the movement of nutrients in the surface film. Detailed study of this rougher surface film has not been thoroughly addressed. A base film is a relatively continuous accumulation of cells and polymer, and is more dense than the surface film. The density and continuity provide a structure that may limit advective transport within the base film. Mass transport of nutrients through the base film is, therefore, likely to be dominated by molecular diffusion. Monopopulation biofilms composed entirely of base films have been observed in high-shear, oligotrophic environments (Wilderer and Characklis, 1989).

MATERIALS AND METHODS

Microbial species and media

A pure culture of *Ps. aeruginosa* was used in these experiments because biofilm kinetic and stoichiometric coefficients have been determined previously (Robinson *et al.*, 1984). Separate vials of the stock culture were maintained in glycerol at −40°C to provide a reproducible inoculum. Bacteria were grown on a minimal-salts medium with glucose as the sole source of carbon and energy. The nutrient medium was identical to that used by Siebel (1987), except that the calcium concentration was lowered to prevent precipitation of calcium phosphate (Peyton and Characklis, 1993). Concentrated micronutrient solutions were prepared in 11-l Nalgene® bottles and autoclaved for 4 h at 121°C. After autoclaving, 20 ml of sterile concentrated glucose solution was added to each micronutrient bottle to give a final glucose concentration of 500 g m^{-3}. Concentrated phosphate buffer solution was prepared in 3.5-l glass containers and autoclaved for 1 h. Dilution water was distilled water filtered through two 0.2-μm (2×10^{-7} m) Gelman cartridge filters. Concentrated micronutrient/glucose and buffer solutions were mixed with dilution water immediately before entering the biofilm reactor. Micronutrient flow rates were adjusted to give the desired influent glucose carbon (GC) concentration of either 0.8, 4.0 or 7.2 g GC m^{-3} with resultant areal substrate loading rates to the reactor of 0.0102, 0.0512, and 0.0922 g GC m^{-2} h^{-1}, respectively. The pH was buffered at 6.7 ± 0.02.

Biofilm reactor

An annular reactor was used because it allowed independent control of shear stress and volumetric flow rate. Torque was measured by the method of Characklis and Roe (1984) to determine average shear stress on the biofilm. Twelve removable coupons allowed direct biofilm sampling without taking the reactor off-line. Draft tubes inside the inner cylinder completely mixed the reactor contents, giving it the characteristics of a continuous stirred tank reactor (Trulear, 1983). A schematic of the reactor and supporting apparatus can be found in Peyton and Characklis (1993). The reactor was disassembled and cleaned before each experiment by scrubbing the reactor and coupons with a brush and hot water containing laboratory glassware soap. Harsh chemicals were not used because of possible residual effects. The thoroughly cleaned reactor was reassembled, autoclaved empty for 0.5 h at 121°C, and allowed to cool. The reactor was filled with nutrients and operated in batch mode at 200 r.p.m. for 24 h. After this initial 24 h, the rotational speed was set to 200 ± 0.3, 302 ± 0.5, or 400 ± 0.6 r.p.m., which resulted in shear stresses of 1.44, 2.20, and 2.97 N m^{-2}, respectively. Liquid flow was then started. This time was defined as experimental time zero. The phosphate buffer flow rate was constant at 24 ml h^{-1} (2.4×10^{-5} m^3 h^{-1}) through all experiments. The glucose/micronutrient solution volumetric flow rate was adjusted to give the desired influent glucose concentration. The flow rate of the dilution water was adjusted to give a total volumetric flow rate of 2.38 l h^{-1}. The resultant residence time of 0.25 h minimized the effects of cellular growth in suspension. Temperature, pH, rotational speed, and torque were continuously logged by computer with a laboratory interface (SCI Technologies, Bozeman, Mont.). Reactor temperature was maintained at 20 ± 0.1°C with a water bath (Neslab, Portsmouth, N.H.). Tests were run for a minimum of 240 hs.

Analytical methods

Glucose. Reactor effluent samples were sterilized with a 0.2-μm cellulose nitrate syringe filter and were analyzed for glucose with the Sigma Diagnostics® enzymatic glucose determination kit (Sigma procedure 510). All glucose samples were frozen immediately after sampling and were analyzed after the experiment was completed.

Biofilm thickness. Biofilm thickness was measured on the coupons with an optical microscope according to the method of Bakke and Olsson (1986). Eight optical-thickness measurements were taken for each coupon removed. The optical thickness is not the same as the actual mechanical thickness because of differences in the reactive index of air and water, therefore, as stated by Bakke and Olsson, a correction factor of 4/3 must be applied. In this paper "biofilm thickness" refers to the average mechanical thickness. The standard deviation of the eight mechanical thickness measurements is defined as the biofilm roughness.

Areal biofilm density. Biofilm was scraped from a known area of a coupon into an aluminum dish of known weight, which had been dried at 104°C overnight. The dish containing biofilm was dried overnight and weighed again to determine dry mass. Volumetric density was calculated by dividing areal density by average biofilm thickness.

Statistical methods

A 3^2 factorial experimental design (Petersen, 1985) was used to determine the effects of substrate loading rate and shear stress on biofilm thickness. Each replication was a separate, independent experiment, resulting in a total of twelve experiments. An advantage of this design was the ability to distinguish the main effects of each factor (shear stress or substrate loading rate) and any possible interactive

Table 3. Summary of results from ANOVA of measured dependent variables at steady state against independent variables of shear stress and substrate loading rate

Variable	*P*-value[a] Substrate loading rate	Shear stress
Biofilm characteristics		
Thickness	<0.0001	0.7945
Roughness	<0.0001	0.0690
Areal mass density	<0.0001	0.0132
Volumetric mass density	0.1268	0.1293

[a]The *P*-value is the probability that the true value of the dependent variable is the same at all three values of the independent variable.

effects. The statistical software package "MSUSTAT" was used for the analysis of variance and multiple regression (MSUSTAT 1986). Significance was determined at the 95% level ($P = 0.05$). Regression analysis was performed assuming that the independent variable, usually biofilm thickness, was error free. In this case however, both variables have associated measurement errors. Data are reported as the mean $\pm$ SE, except in describing biofilm roughness, where the standard deviation of the biofilm thickness was used. The standard error of biofilm thickness does not directly reflect the roughness.

RESULTS

Table 3 gives the results of the statistical analysis of the effects of shear stress and the substrate loading rate on variables that characterize biofilm accumulation. At a 95% confidence interval, the substrate loading rate significantly affected all variables except the volumetric mass density; shear stress had no significant effect, except on areal mass density.

Biofilm thickness

Figure 1 depicts a typical time progression of the average biofilm thickness at the three levels of substrate-loading rates. Data for Fig. 1 are taken from tests run at a shear stress of 1.44 Nm^{-2} (200 r.p.m.). The biofilm thickness increased rapidly and leveled off at the steady state value. Steady state thickness with substrate loading rate and shear stress is given in Fig. 2. Thickness increased significantly with increases in substrate loading rate and showed no consistent response to increasing shear stress.

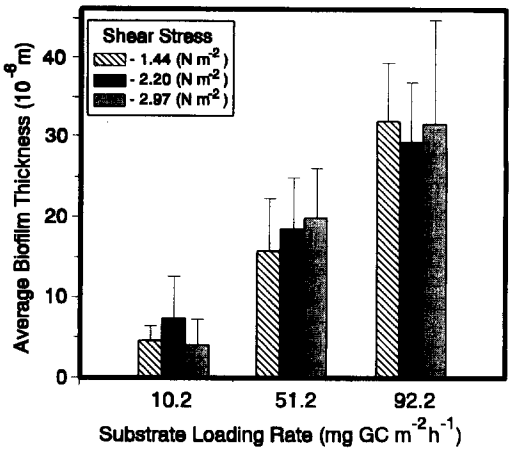

Fig. 2. Steady state biofilm thickness increased with substrate loading rate. Shear stress had no significant effect. Error bars are standard deviation of 8–40 measurements and are indicative of the roughness of the biofilm.

Biofilm roughness

Figure 3, which combines data from all experiments, shows that biofilm roughness increased with thickness. The slope of 0.22 $\pm$ 0.02 (unitless) indicates that roughness was approx. 20% of the measured average thickness. Statistical analysis indicates that substrate-loading rate significantly influenced roughness (Table 3). No significant or consistent dependence on shear stress was observed.

Areal and volumetric mass density

Areal mass density, X_f (kg m^{-2}), increased with substrate loading rate (Fig. 4) and therefore increasing biofilm thickness, L_f (Fig. 5). Although statistics suggest that shear stress had a significant influence in areal mass density (*P*-value = 0.0132), no consistent trend was found. Regression of areal mass density data was performed with both a first order model in

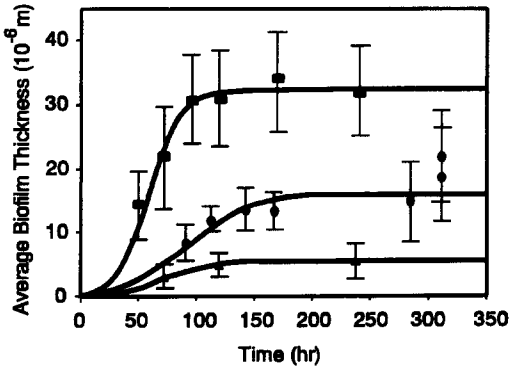

Fig. 1. Typical time-progression of the average *Ps. aeruginosa* biofilm thickness for three levels of substrate loading rate (▲: 10.2; ●: 51.2; ■: 92.2 mg GC m^{-2} h^{-1}).

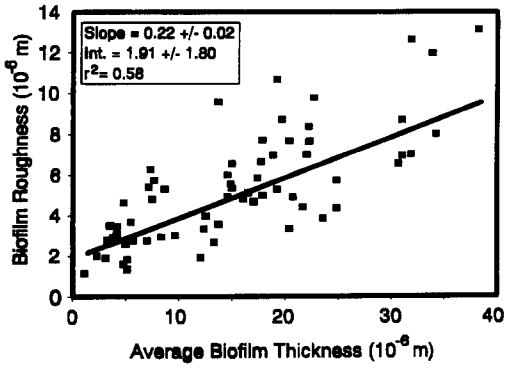

Fig. 3. *Ps. aeruginosa* biofilm roughness was approximately one-fifth of the measured average biofilm thickness.

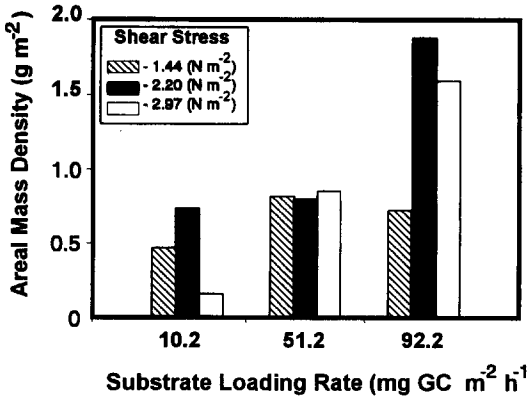

Fig. 4. Steady state areal mass density increased with increasing substrate loading rate, but showed no consistent pattern with varied shear stress.

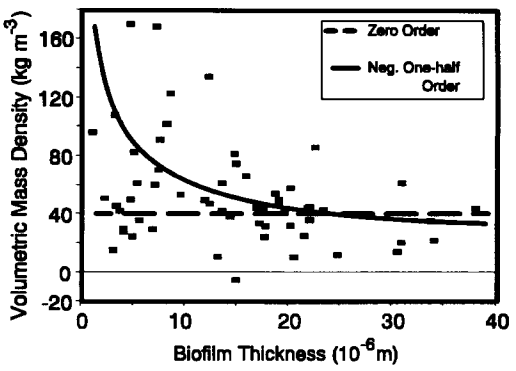

Fig. 6. Volumetric mass density decreased with increasing average biofilm thickness. Lines are calculated from equations (5) and (6), giving zero and negative one-half order expressions in biofilm thickness.

biofilm thickness [equation (1)] which assumes a constant volumetric mass density and a one-half order model in biofilm thickness [equation (2)]

$$X_f = k_{\rho 1} L_f \quad (1)$$

$$X_f = k_{\rho 1/2} \sqrt{L_f}. \quad (2)$$

The regression coefficients determined were 39.5 ± 3.11 ($kg\,m^{-3}$) for the first order model [equation (1)], and 0.199 ± 0.041 ($kg\,m^{-5/2}$) for the one-half order model [equation (2)], but both gave low squared correlation coefficients, 0.17 and 0.29, respectively.

The volumetric mass density decreased with increasing thickness (Fig. 6). The significance of the relationship between thickness and volumetric mass density was determined with a linear regression. The slope of the line was -1.31 $kg/m^3/\mu m$, with a 95% confidence interval (-2.63, -0.31), indicating that the slope of the line is significantly different from zero. The lines on Fig. 6 were calculated from the regressions of the areal mass density [equations (1) and (2)] and thickness. The observed decrease in volumetric mass density with increasing substrate loading rate (P-value = 0.12) was insignificant at the 95% level. No consistent or significant influence of shear stress was observed. Both models gave accurate predictions of volumetric mass density for biofilm thicknesses greater than 15 μm, however, systematic deviations in the residuals (measured–calculated) were observed. The first order model had an average residual volumetric density of 15.67 kg/m^3, whereas the negative one-half order model had an average residual of -9.89 kg/m^3.

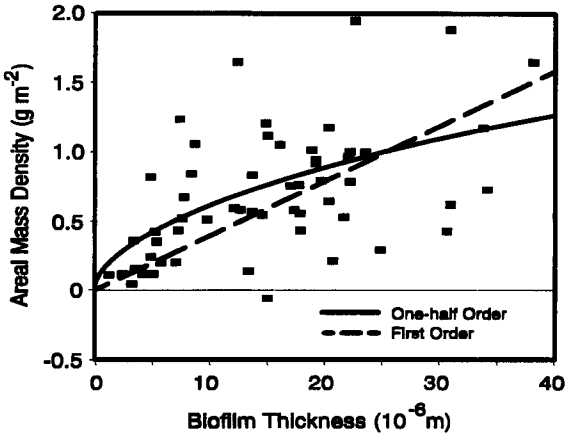

Fig. 5. Areal mass density increased with increasing biofilm thickness. First order and one-half order regression lines are plotted. These regressions give squared correlation coefficients of 0.17 and 0.29, respectively.

DISCUSSION

Biofilm thickness

Steady state biofilm thickness is dependent on the substrate-loading rate. Average steady state values for measured thicknesses were 6.20, 17.61 and 31.85 μm (10^{-6} m) for substrate loading rates of 10.2, 51.2 and 92.2 mg GC $m^{-2}\,h^{-1}$, respectively. This indicates that biofilm thickness is dependent on substrate loading rate between 10.2 and 92.2 mg GC $m^{-2}\,h^{-1}$. Data on *Ps. aeruginosa* biofilm thickness at such low substrate loading rates (10.2 mg GC $m^{-2}\,h^{-1}$) were not available before this research. Previous research (Trulear 1983; Siebel 1987) with *Ps. aeruginosa* in an annular reactor found that the average steady state biofilm thickness was approximately 33 μm (3.3×10^{-5} m), and the lowest reported substrate loading rate was 65.3 mg GC $m^{-2}\,h^{-1}$. In most of these experiments the substrate utilization rate was nearly equal to the substrate loading rate. Figure 7 shows that the steady state thickness increases with substrate utilization rate up to approximately 120 mg GC $m^{-2}\,h^{-1}$ and then levels off at 33 μm (3.3×10^{-5} m). It is not clear why the average plateau thickness for *Ps. aeruginosa* is in this range. In mixed populations, biofilm thicknesses are typically an

order of magnitude higher at identical substrate-loading rates and rotational speeds (Peyton, 1992); thus the strength of EPS bonds between cells and to the substratum, and the general biofilm structure may be key variables that determine thickness.

Biofilm roughness

Data on biofilm roughness may provide insight for microscale computer modelling efforts. The standard deviation of the *Ps. aeruginosa* biofilm thickness is approximately one-fifth (0.22) of the mean biofilm thickness (Fig. 3). For a normal distribution of measured thickness values, approximately 95% would fall within 2 SD of the mean. As an example, for a 30 μm (3.0×10^{-5} m) average film thickness, individual measurements would typically be in the range of 18–42 μm (1.8×10^{-5} to 4.2×10^{-5} m). No existing models account for film roughness and the differences in fluid dynamics and mass transfer that may result. Rougher films would likely have higher mass transfer coefficients than smoother films, and thus would result in a higher growth rate for a given bulk-liquid substrate concentration. Mixed population biofilm roughness observed by Peyton (1992) sometimes exceeded the mean value of biofilm thickness. Thus, not only are mixed culture biofilms thicker, but their morphology is much more heterogeneous.

Areal and volumetric mass density

For modelling purposes, it would be useful to obtain correlations which account for the changes in structure as the biofilm ages and matures. The areal mass density was fit with both a first order [equation (1)] and one-half order [equation (2)] expression in average thickness (Fig. 5). The regression analysis gave low squared correlation coefficients (r^2) of 0.29 and 0.17, respectively. From these regressions, the volumetric mass density (calculated by dividing areal density by the thickness) can be plotted against the observed values. Fitting the areal mass density with a first order regression in film thickness (Fig. 5) results in a zero order, or constant volumetric mass density, ρ_f [equation (3)].

$$\rho_f = k_{\rho 1} \tag{3}$$

$$\rho_f = \frac{k_{\rho 1/2}}{\sqrt{L_f}}. \tag{4}$$

Also, fitting the areal mass density with a one-half order expression in biofilm thickness gives a negative one-half order expression in film thickness for volumetric mass density [equation (4)]. Solving equation (4) for a monolayer of cells $L_{fm} = 1.0\ \mu$m (1×10^{-6} m) gives a value of $\rho_{fm} = 199 \pm 41$ kg m^{-3} for the volumetric density of the first layer of cells attached to the substratum. Wanner (1989) reported a monolayer volumetric density of 200 kg m^{-3}.

Most biofilm models assume constant volumetric mass density [equation (3)] (Howell and Atkinson, 1976; Rittmann and McCarty, 1978, 1980, 1981; Wanner and Gujer, 1986; Chang and Rittmann, 1987, 1988; Namkung and Rittmann, 1987; Suidan *et al.*, 1987; Skowlund and Kirmse, 1989). Although certainly not conclusive, the data from this study suggest that volumetric mass density may be better modelled with a negative one-half order expression in biofilm thickness [equation (4)]. In contrast to equation (3), equation (4) predicts high volumetric density values for thin films and low density values for thicker films.

As an extension of this regression analysis, the *local* volumetric mass density, ρ_{fz}, can be calculated with biofilm depth. Local biofilm density is defined as the density at a specific location in the biofilm, as opposed to typically measured density values that are the average density over the entire biofilm thickness. Using the calculus definition of an average

$$\rho_f = \frac{\int_0^{L_\rho} \rho_{f_z}\, dz}{\int_0^{L_\rho} dz}. \tag{5}$$

Integrating the demoninator and substituting equation (4) gives

$$k_{\rho 1/2}\sqrt{L_f} = \int_0^{L_\rho} \rho_{f_z}\, dz. \tag{6}$$

Solving equation (6) for ρ_{fz} gives the final form of the local density profile with depth in the biofilm [equation (7)].

$$\rho_{f_z} = \frac{k_{\rho 1/2}}{2\sqrt{z}}. \tag{7}$$

Equation (7) predicts that the high density of the deeper biofilm layers have a large effect on the average volumetric density (Fig. 8). Further volumetric mass density data are required to verify and refine this approach, since different biofilms may have different values of $k_{\rho 1/2}$. Even so, this model is qualitatively consistent with the changes in volumetric

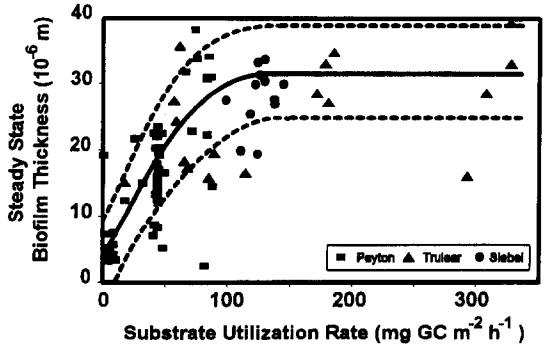

Fig. 7. Steady state biofilm thickness from this study combined with that of Trulear (1983) and Siebel (1987). Thickness increased with increasing substrate utilization rates up to ~120 mg GC m^{-2} h^{-1} where average biofilm thickness plateaued at ~33 μm. Dashed lines indicate 95% confidence interval of the mean.

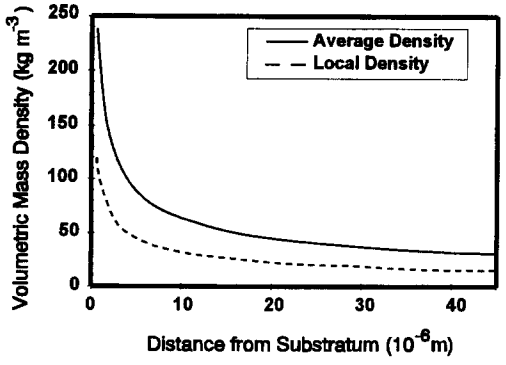

Fig. 8. Predicted average and local volumetric mass density from equations (4) and (9), respectively.

density with depth measured by Masuda *et al.* (1991) (Table 2). Their data indicate that the average volumetric density of the total biofilm was 65.3 dry kg wet m^{-3}.

This analysis is intended to describe a conceptual approach to modelling biofilm volumetric density and is based on intrinsically noisy measurements of thickness and areal mass density. Analytical errors are more likely to occur when measuring the density of thinner films, since a small absolute error in the biofilm thickness measurement may lead to a large error in the calculated volumetric density.

CONCLUSIONS

The results of this research indicate that, over the range of variables tested:

1. Increases in substrate loading rate significantly increase steady state biofilm thickness up to an average of 33 microns for monopopulation *Ps. aeruginosa* biofilms. Literature data indicate, however, that substrate loading rates exceeding 120 mg GC $m^{-2} h^{-1}$ do not further increase the steady state biofilm thickness. No significant effect of shear stress on thickness was observed over the range of shear stress tested.

2. Biofilm roughness, as measured by the standard deviation of thickness, increases with increasing thickness. Linear regression indicates that roughness is $22 \pm 2\%$ of the *Ps. aeruginosa* biofilm thickness.

3. Areal mass density significantly increased with substrate loading rate. Although ANOVA indicated a significant effect ($P = 0.0132$) of shear stress on areal mass density, no consistent trend was observed. Areal mass density was described as a function of thickness equally well by a first order or a one-half order expression.

4. Volumetric mass density was not significantly affected by substrate loading or shear stress. Decreases in volumetric mass density with biofilm depth have been reported in the literature and can be calculated with a negative one-half order expression for volumetric mass density.

Acknowledgements—The author gratefully acknowledges guidance and technical support from Bill Characklis and financial support from Conoco, Inc., and the National Science Foundation Engineering Research Center Program. This article was reviewed and published with support from the U.S. Department of Energy, Office of Technology Development VOC Arid Integrated Demonstration. Dr. Rodney Skeen kindly provided editorial comments.

REFERENCES

Bakke R., Trulear M. G., Robinson J. A. and Characklis W. G. (1984) Activity of *Pseudomonas aeruginosa* in biofilms: steady state. *Biotechnol. Bioengng* **26,** 1418–1424.

Bakke R. and Olsson P. Q. (1986) Biofilm thickness measurements by light microscopy. *J. Microbiol. Meth.* **5,** 93–99.

Bryers J. and Drummond F. (1995) Diffusion coefficients in structurally non-uniform hydrogels: mass transfer in bacterial biofilms. *Biotechnol. Bioengng*. Submitted.

Chang H. T. and Rittmann B. E. (1987) Mathematical modeling of biofilm on activated carbon. *Environ. Sci. Technol.* **21,** 273–279.

Chang H. T. and Rittmann B. E. (1988) Comparative study of biofilm shear loss on different adsorptive media. *J. Wat. Pollut. Control Fed.* **60,** 362–368.

Chang H. T., Rittmann B. E., Amar D., Heim R., Ehlinger O. and Lesty Y. (1991) Biofilm detachment mechanisms in a liquid-fluidized bed. *Biotechnol. Bioengng* **38,** 499–506.

Characklis W. G., Bryers J. D., Trulear M. G. and Zelver N. (1980) Biofouling film development and its effects on energy losses: a laboratory study. In *Condenser Biofouling Control* (Edited by Garey J. F. *et al.*) Ann Arbor Science, Ann Arbor, Mich.

Characklis W. G. and Roe F. L. (1984) Monitoring buildup of fouling deposits on surfaces of fluid handling systems. U.S. Patent 4,485,450.

Christensen B. E. and Characklis W. G. (1990) Physical and chemical properties of biofilms. In *Biofilms* (Edited by Characklis W. G. and Marshall K. C.), pp. 93–130. Wiley, New York.

Cunningham A. B. (1989) Hydrodynamics and solute transport at the fluid-biofilm interface. In *Structure and Function of Biofilms* (Edited by Characklis W. G. and Wilderer P. A.), pp. 19–31. Wiley, New York.

Duguid I. G., Evans E., Brown M. R. W. and Gilbert P. (1992) Effect of Biofilm Culture upon the Susceptibility of *Staphylococcus epidermidis* to Tobramycin. *J. Antimicrob. Chemother.* **30,** 803–810.

Gagnon R. F. and Richards G. K. (1993) A mouse model of implant-associated infection. *Int. J. artif. Organs* **16,** 789–798.

Geesey G. G., Mittelman M. W. and Lieu V. T. (1987) Evaluation of slime-producing bacteria in oil field core flood experiments. *Appl. environ. Microbiol.* **53,** 278–283.

Howell J. A. and Atkinson B. (1976) Sloughing of microbial film in trickling filters. *Wat. Res.* **10,** 307–315.

Jennings D., Peterson J. N., Skeen R. S., Hooker B. S., Peyton B. M. and Johnstone D. L. (1995) Effects of slight variations in nutrient loadings on pore plugging. *Appl. biochem. Biotechnol.* **52,** 727–734.

Kornegay B. H. and Andrews J. F. (1967) Characteristics and kinetics of fixed film biological reactors. Final Report, Grant WP-01181, Federal Water Pollution Control Administration, U.S. GPO, Washington, D.C.

LeChevallier M. W., Babcock T. M. and Lee R. G. (1987) Examination and characterization of distribution system biofilms. *Appl. environ. Microbiol.* **53,** 2714–2724.

LeChevallier M. W., Schulz W. and Lee R. G. (1991) Bacterial nutrients in drinking water. *Appl. environ. Microbiol.* **57,** 857–862.

Masuda S., Watanabe Y. and Ishiguro M. (1991) Biofilm properties and simultaneous nitrification and denitrification in aerobic rotating biological contractors. *Wat. Sci. Technol.* **23,** 1355–1363.

MSUSTAT Statistical Analysis Package Version 3.20 (1986) Developed by Richard E. Lund, Montana State University, Bozeman, Mont.

Mulcahy L. T. and Shieh W. K. (1987) Fluidization and reactor biomass characteristics of the denitrification fluidized bed biofilm reactor. *Wat. Res.* **21,** 451–458.

Namkung E. and Rittmann B. E. (1987) Modeling bisubstrate removal by biofilms. *Biotech. Bioengng* **29,** 269–278.

Norrman G., Characklis W. G. and Bryers J. D. (1977) *Dev. Ind. Microbiol.* **18,** 581.

Olsson J., Van der Heijde Y. and Holmberg K. (1992) Plaque formation *in-vivo* and bacterial attachment *in-vitro* on permanently hydrophobic and hydrophilic surfaces. *Caries Res.* **26,** 428–433.

Petersen R. G. (1985) *Design and Analysis of Experiments.* Marcel Dekker, New York.

Peyton B. M. (1992) Kinetics of biofilm detachment. Ph.D. thesis, Montana State Univ., Bozeman, Mont.

Peyton B. M. and Characklis W. G. (1993) A statistical analysis of the effect of substrate utilization and shear stress on the kinetics of biofilm detachment. *Biotechnol. Bioengng* **41,** 728–735.

Picologlou B. F., Zelver N. and Characklis W. G. (1980) Biofilm growth and hydraulic performance. *J. Hydraul. Division, Proc. ASCE* **106**(HY5), 733–746.

Richards G. K. and Gagnon R. F. (1993) An assay of *Staphylococcus epidermidis* biofilm responses to therapeutic agents. *Int. J. Artif. Organs* **16,** 777–787.

Rittmann B. E. and McCarty P. L. (1978) Variable-order model of bacterial-film kinetics. *J. Environ. Engng Division, Proc. ASCE* **104**(EE5), 889–900.

Rittmann B. E. and McCarty P. L. (1980) Model of steady-state biofilm kinetics. *Biotechnol. Bioengng* **22,** 2343–2357.

Rittmann B. E. and McCarty P. L. (1981) Substrate flux into biofilms of any thickness. *J. Environ. Engng Division, Proc. ASCE* **107**(EE4), 831–849.

Robinson J. A., Trulear M. G. and Characklis W. G. (1984) Cellular reproduction and extracellular polymer formation by *Pseudomonas aeruginosa* in continuous culture. *Biotechnol. Bioengng* **26,** 1409–1417.

Saberiyan A. G., Wilson M. A., Roe E. O., Andrilenas J. S., Esler C. T., Kise G. H. and Rieth P. E. (1994) Removal of gasoline volatile organic compounds via air biofiltration: a technique for treating secondary air emissions from vapor-extraction and air-stripping systems. In *Hydrocarbon Bioremediation* (Edited by Hinchee R. E, Alleman B. C., Hoeppel R. E. and Miller R. N.), pp. 1–12. Lewis, Ann Arbor, Mich.

Sanders W. M. III (1964) The relationship between oxygen utilization of heterotrophic slime organisms and the wetted perimeter, Ph.D. thesis, John Hopkins Univ., Baltimore, Md.

Semprini L., Hopkins G. D., Janssen D. B., Lang M., Roberts P. V. and McCarty P. L. (1991) *In situ* biotransformation of carbon tetrachloride under anoxic conditions. EPA Report No. EPA 2-90/060, US EPA, Ada, Okla.

Shields M. S., Reagin M. J., Gerger R. R., Sommerville C., Schaubhut R., Campbell R. and Hu-Primmer J. (1994) Constitutive degradation of trichloroethylene by an altered bacterium in a gas-phase reactor in *Bioremediation of Chlorinated and Polycyclic Aromatic Hydrocarbon Compounds* (Edited by Hinchee R. E., Leeson A., Semprini L. and Ong S. K.), pp. 50–65. Lewis, Ann Arbor, Mich.

Siebel M. A. (1987) Binary population biofilms, Ph.D. Thesis, Montana State University, Bozeman, Mont.

Skowlund C. T. and Kirmse D. W. (1989) Simplified models for packed-bed biofilm reactors. *Biotechnol. Bioengng* **33,** 164–172.

Shouche M., Petersen J. N. and Skeen R. S. (1993) Use of a mathematical model for prediction of optimum feeding strategies for *in situ* bioremediation. *Appl. Biochem. Biotechnol.* **39,** 763–779.

Suidan M. T., Rittmann B. E. and Traegner U. K. (1987) Criteria establishing biofilm-kinetic types. *Wat. Res.* **21**(4), 491–498.

Suschka J. (1987) Hydraulic performance of percolating biological filters and consideration of oxygen transfer. *Wat. Res.* **21,** 865.

Trulear M. G. (1983) Cellular reproduction and extracellular polymer formation in the development of biofilms. Ph.D. thesis, Montana State University, Bozeman, Mont.

Turakhia M. and Characklis W. G. (1983) An observation of microbial cell accumulation in a finned tube. *Can. J. Chem. Engng* **61,** 873–875.

van der Wende E., Characklis W. G. and Smith D. B. (1989) Biofilms and bacterial drinking water quality. *Wat. Res.* **23,** 1313–1322.

Voice T. C., Pak D., Zhao X., Shi J. and Hickey R. F. (1992) Biological activated carbon in fluidized bed reactors for the treatment of groundwater contaminated with volatile aromatic hydrocarbons. *Wat. Res.* **26,** 1389–1401.

Wanner O. and Gujer W. (1986) A multispecies biofilm model. *Biotechnol. Bioengng* **28,** 314–328.

Wanner O. (1989) Modeling population dynamics. In *Structure and Function of Biofilms* (Edited by Characklis W. G. and Wilderer P. A.), pp. 91–110. Wiley, New York.

Wilderer P. A. and Characklis W. G. (1989) Structure and function of biofilms. In *Structure and Function of Biofilms* (Edited by Characklis W. G. and Wilderer P. A.), pp. 5–17. Wiley, New York.

Wilson L. A., Sawant A. D., Simmons R. B. and Ahearn D. G. (1990) Microbial contamination of contact lens storage cases and solutions. *Am. J. Ophthalmol.* **110,** 193–198.

Wuhrmann K. (1971) Stream purification. In *Water Pollution Microbiology.* (Edited by Mitchell R.), Wiley, New York.